Clinical and Translational Radiation Oncology 24 (2020) 116–122

Contents lists available at ScienceDirect

Clinical and Translational Radiation Oncology

journal homepage: www.elsevier.com/locate/ctro

In-vivo and *in-vitro* impact of high-dose rate radiotherapy using flattening-filter-free beams on the anti-tumor immune response

P.A. Laurent [a], A. Kownacka [a], R. Boidot [b], C. Richard [b,c], E. Limagne [b,c], V. Morgand [a], L. Froidurot [a], C. Bonin [d], L. Aubignac [d], F. Ghiringhelli [b,c,e], G. Créhange [a], C. Mirjolet [a,c,*]

[a] Department of Radiation Oncology, Unicancer – Georges-Francois Leclerc Cancer Center, Dijon, France
[b] Cancer Biology Research Platform, Unicancer – Georges-Francois Leclerc Cancer Center, Dijon, France
[c] INSERM UMR 1231, Dijon, France
[d] Department of Medical Physics, Unicancer – Center Georges-Francois Leclerc, Dijon, France
[e] Department of Medical Oncology, Unicancer – Center Georges-Francois Leclerc, Dijon, France

ARTICLE INFO

Article history:
Received 30 April 2020
Revised 15 July 2020
Accepted 20 July 2020
Available online 31 July 2020

Keywords:
Radio-induced immune response
Dose rate modulation
Flattening filter free

ABSTRACT

Introduction: Modern accelerators have the "flattening filter-free" (FFF) technique to deliver RT with a moderate high-dose rate, currently used in limited clinical indications. No scientifically established data are currently available on the possible effects of this high dose rate on the anti-tumor immune response. We therefore propose here to study these effects in a preclinical CT26 murine colorectal tumor model.
Material and methods: *In-vitro*, CT26 cells were irradiated on a Varian TrueBeam® linac at 3 different dose rates (4; 12 or 24 Gy/min) using the FFF mode. Activation of the anti-tumor immune response was evaluated by the analysis of induction of genes of the type I interferon pathway by RT-qPCR, and by the study of the induction of immunogenic death biomarkers. *In-vivo*, an efficacy study of RT delivering 16.5 Gy at 2 different dose rates was performed in immunocompetent Balb/c mice carrying CT26 syngeneic tumors, as well as an immunomonitoring analysed by flow cytometry and a transcriptomic analysis using RNA sequencing. Statistical analyzes were performed using non-parametric tests.
Results: *In-vitro,* no significant influence of an increase in FFF dose rate was shown for the induction of genes of the type I interferon pathway as well as for the studied immunogenic death markers (HMGB1 secretion). *In-vivo*, no difference in terms of tumor growth retardation between the 2 dose rates used was demonstrated, as well as for the composition of immune cell infiltrates within tumor microenvironment and the expression of immune checkpoints in immunomonitoring and RNAseq.
Conclusion: In this study involving the CT26 model, no influence of a moderate high dose rate in FFF technique on the anti-tumor immune response was demonstrated, which would make studies of associations between RT and checkpoint inhibitors fit with this technique of RT. However, further explorations using other cellular models seem to be of interest.

1. Introduction

Mainly considered in case of contraindication to a surgical curative treatment [1,2] or for treatment of a low-number of metastases [3], hypofractionation and ablative strereotactic body radiotherapy (SBRT), helped by recent technical advances, have been notably implemented in daily practice. This growing interest is however counterbalanced by the subsequent increase in time dedicated to deliver the treatment in this setting, especially in a current context of global lack of resources [4].

Indeed, delivering high doses of radiotherapy (RT), such as those of 8 to 24 Gy delivered in ablative SBRT, with a conventional dose-rate, is time-consuming both in terms of time for treatment delivery and for repositioning procedures within the framework of required image-guided radiotherapy (IGRT) [5]. One way to handle this issue is the use of flattening-filter-free (FFF) technique, consisting in removing flattening-filter from Linac and thereby increasing dose rate by ~ 4 times (~2000 MU/minute versus ~ 500 MU/minute) in a non-uniform dose profile beam characterized by reduced head scatter, leaf transmission, energy variation in a lateral direction and reduced peripheral dose in comparison with flattened beam (FB) [6]. This decreases beam-on

* Corresponding author at: Research team of Radiobiology, Preclinical and Translational Radiotherapy, Department of Radiation Oncology, Georges-François Leclerc Cancer Centre, 1 rue Professeur Marion, BP 77 980, 21079 DIJON Cedex, France.
E-mail address: cmirjolet@cgfl.fr (C. Mirjolet).

https://doi.org/10.1016/j.ctro.2020.07.004

time (BOT), resulting in shortening time of RT sessions with the effect to minimize deleterious intra-fraction motion involving patient and/or tumor, thereby increasing reliability of initial treatment planification [7].

On one hand, RT has shown its ability to generate an immune response against tumor, requiring the help of several immune cell subtypes, such as T lymphocytes (CD4 + or CD8 +) or Natural Killers (NK) [8]. One side of this response is the generation of immune cell death (ICD) events recognizable, *inter alia,* by high mobility group box 1 protein (HMGB1) secretion [9]. RT can also act on tumor microenvironment by modifying its cytokine expression profile, favoring the secretion of type I interferons and by the way the subsequent products of interferon-stimulated-genes (ISG), for example C-X-C motif ligand 10 (CXCL10) and interferon-induced GTP-binding protein MX1, thus encouraging the recruitment and function of effector T CD8 + cells with a substantial antitumoral effect [10–12].

On the other hand, under certain fractionation regimens, RT can also enhance immunosuppressive effects such as the induction of TREX1 exonuclease which can censor type I interferons induction [13]. Moreover, it is able to improve the recruitment of T regulators lymphocytes (Tregs) [14] and myeloid-derived suppressor cells (MDSC) within tumor microenvironment [15]. Finally, as we have recently demonstrated it, RT is capable of inducing expression of immune checkpoints depending on fractionation schedule, thus paving the way to interesting combinations between RT and immune-checkpoints blockades (ICB) [16].

Clinical applications of FFF remain controversial, as observations about its efficacy and safety may differ according to several preclinical studies. Indeed, some of them did not show any significant difference in cell survival in different populations (healthy or cancer cell lines) irradiated in conventional dose rate or in high dose rate [17–20], whereas some others may indicate a preference for RT delivered in high-dose rate FFF regarding tumor-cell death and healthy tissue sparing [21]. Based on these findings, FFF is a technique already experienced in clinical settings in SBRT of vertebral, lung, liver or intracranial tumors in order to decrease the time dedicated to treatment and optimize available resources [22].

In a current era of exponential development of combination treatments involving RT with concurrent administration of immune therapies, there is a critical need to ensure that new RT modalities, such as FFF RT, will not be deleterious for the induction of an anti-tumor immune response following RT. However, despite evidence is showing an equivalence in terms of cell death and of toxicity to healthy tissues of RT delivered in high-dose rate using FFF compared to conventional dose-rate, it exists a severe lack of data exploring the potential effects of this RT modality on anti-tumor immune response. This paper therefore discusses these potential effects by exploring primordial pathways involved in anti-tumor immune response in a CT26-based model, irradiated *in-vitro* and *in-vivo* whether in high-dose rate using FFF or in conventional dose-rate.

2. Material and methods

2.1. In-vitro study

2.1.1. Cell culture and irradiation

CT26 American Type Culture Collection (ATCC) murine colon cancer cells (USA) were cultured with the same conditions as those used according to previous works[16]. A total of 1.10^5 CT26 cells were transferred in 13 different 6-well plates (including a control un-irradiated plate), and then irradiated, using a TrueBeam® linear accelerator delivering a single 10x10 cm FFF beam, with a single dose of 2, 5, 8 or 12 Gy each delivered with a dose rate of 4 (LDR group), 12 (HDR1 group) or 24 Gy/min (HDR2 group). An overview of the planified dosimetry is available in Supplementary Fig. 1.

2.1.2. RT-qPCR

As previously described [23], 48 h after RT, we quantified in RT-qPCR the expression of *trex1* (coding for exonuclease TREX1, antagonist of type I interferon pathway) and interferon I-stimulated genes (ISG) *ifnb* (interferon β), *ifnar1* (type I interferon receptor), *cxcl10* (chemokine CXCL10) and *mx1* (MX1). Primers used are detailed in Supplementary Table 1. Relative quantities were calculated in arbitrary units (UA) using the ΔCT method and the following formula: $2(-\Delta CT).10^4$ with gene *actb* as a gene of reference. The time point of 48 h after RT was chosen because preliminary data from our team showed a relative peak in the expression of some ISG in the CT26 model 48 h after RT, whereas no significant induction was observed 24 h after RT for the same genes.

2.1.3. Immune cell death: HMGB1 secretion

Two days after CT26 irradiation, 400 μL of culture supernatant was harvested for each condition, and concentration of *high-mobility group box protein 1* (HMGB1) was quantified using ELISA kit (Chondrex®) HMGB1 detection kit, ref. 6010 (Redmond, USA)), already involved in the detection and the quantification of HMGB1 in the supernatants of cancer cells [24] as well as of normal cells [25] in published works. A plate-reader Spark® (Tecan™) with a reference wavelength of 450 nm was used.

2.2. In-vivo study

2.2.1. Tumor-growth profile experiments

Immunocompetent Balb/c mice housing and *in-vivo* experiments were performed as previously described [16].

Ten days after sub-cutaneous injection of 1.10^5 CT26 cells on right flank, mice were randomized in three groups: an un-irradiated control group (Control), a high-dose rate group (“HDR”) receiving a single-dose of 16.5 Gy in a high-dose rate of 24 Gy/min and a low-dose rate group (“LDR”) receiving the same single-dose in a low-dose rate of 4 Gy/min. This irradiation scheme was chosen because of its ability to modify tumor microenvironment and induce some relevant anti-tumor immune pathways [16]. An overview of setup and dosimetry is visible on Fig. 1.

The full *in-vivo* research process was approved by competent ethics committee before any experimentation was performed.

2.2.2. Immunomonitoring experiments

After randomization, three other groups of mice were treated either with a single dose of 16.5 Gy delivered at LDR or FFF HDR, or didn’t receive any RT (control group).

Seven days after irradiation, all mice were sacrificed and tumors collected. For each group, 5 tumors were used to analyze cell infiltrates within tumor microenvironment using flow cytometry, whereas the 5 others were used to study the expression of a wide array of genes involved in anti-tumor immune processes using RNA sequencing (see below). The time point of 7 days after irradiation as well as the dose of 16.5 Gy were chosen because of previous works published by our research team showing an induction of anti-tumor immune response with this dose at this time point in CT26 model [16].

2.2.3. Immunomonitoring using flow cytometry:

Tumor microenvironment analyzes were performed as previously described [16]. After dissection, and mechanical then enzymatical dissociation using a mouse tumor dissociation kit and according to manufacturer’s recommendation (Miltenyi Biotech™), tumor cell suspension (10^6 cells) was stained in flow cytometry staining buffer (FSB, eBioScience™) with specific antibodies

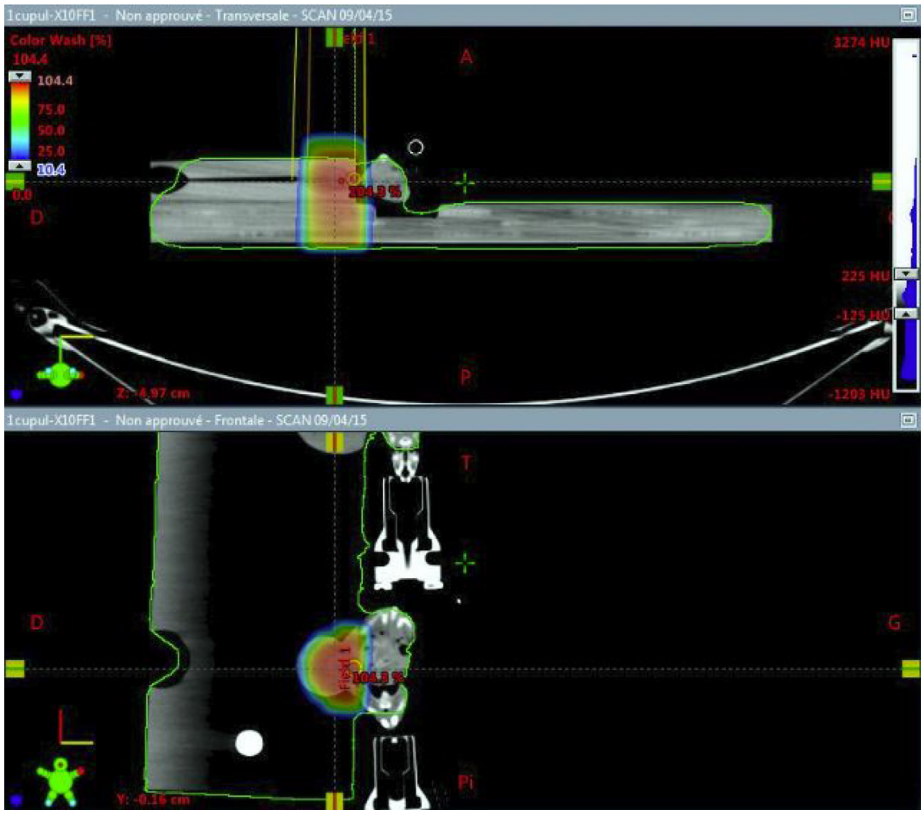

Fig. 1. Setup modalities for Balb/c mice irradiations on Varian™ Truebeam® linear accelerator. RT delivery on tumor alone using a single FFF beam of 10 MV. A home-made contention device immobilized the CT26 tumor located on right-flank of each mice.

according to manufacturer's recommendation, then washed and analyzed using flow cytometry (modalities summarized in Supplementary Table 1).

2.2.4. RNA-sequencing

For RNAseq experiments, we used the same technical modalities and the same hardware devices as those used in similar works published by our team [16].

A gene set enrichment analysis was performed as reported in a previous study [26] using the online software GenePattern based on 2019 KEGG database.

2.3. Statistics and graphical representation

All figures were produced using GraphPad Prism software version 7.0 (Graphpad Software™, USA) Comparisons between the different experimental conditions were performed using a non-parametric Mann-Whitney test. In case of multiple groups which are all compared to each other, a Kruskall-Wallis test (KW) was first performed, and in case of positivity of KW test (threshold $p < 0.05$), a Mann-Whitney non-parametric test was then practiced in a side-by-side comparison, with a post-hoc correction using the method of Benjamini and Hochberg. Statistical analyzes were performed using SAS version 9.4 (SAS Institute Inc., Cary, NC, USA). A p-value < 0.05 was considered to be statistically significant.

3. Results

3.1. In-vitro conditions

3.1.1. Influence of RT dose-rate on the induction of type I interferon pathway

The results of RT-qPCR experiments are detailed in Table 1 and represented in Fig. 2.

Table 1
Effect of RT delivered using three different dose-rate conditions on the expression of genes of the type I interferon pathway.

	trex1	*cxcl10*	*ifnb*	*ifnar1*	*mx1*
Control	35.37 [19.93; 43.75]	18.53 [5.73; 27.3]	0.175 [0.127; 0.325]	82.45 [58.2; 93.53]	1.55 [1.18; 2.1]
LDR (4 Gy/min)	61.61 [39.23; 91.37]	62.41 [23.33; 160.8]	0.51 [0.30; 1]	77.27 [46.14; 96.89]	28.53 [8.63; 38.2]
HDR1 (12 Gy/min)	57.32 [39.06; 74.89]	46.26 [20.76; 130.5]	0.38 [0.23; 0.62]	68.29 [54.03; 85.31]	22.3 [4.31; 35.89]
HDR2 (24 Gy/min)	68.15 [37.92; 84.98]	58.68 [33.08; 110.8]	0.47 [0.35; 0.63]	77.37 [65.72; 87.97]	20.18 [9.82; 37.12]
KW Test	**p = 0.042**	**p = 0.045**	**p = 0.01**	p = 0.79	**p = 0.001**
LDR VS HDR1	p = 0.71	p = 0.81	p = 0.08		p = 0.85
LDR VS HDR2	p = 0.90	p = 0.81	p = 0.47		p = 0.86
HDR2 VS HDR1	p = 0.62	p = 0.64	p = 0.29		p = 0.99
LDR VS Control	**p = 0.008**	**p = 0.01**	**p = 0.002**		**p < 0.001**
HDR1 VS Control	**p = 0.02**	**p = 0.01**	**p = 0.046**		**p < 0.001**
HDR2 VS Control	**p = 0.006**	**p = 0.006**	**p = 0.007**		**p < 0.001**

Results of RTqPCR experiments 48 h after irradiation of *in-vitro* CT26 cells. All results represented in medians with interquartile ranges of arbitrary units (n = 6). Data comparison made using a Kruskall-Wallis (KW) test, and then a Mann-Whitney non-parametric test with correction of Benjamini and Hochberg in case of significance of KW test. LDR: Low-dose rate; HDR1: High-dose rate 1; HDR2: High-dose rate 2.

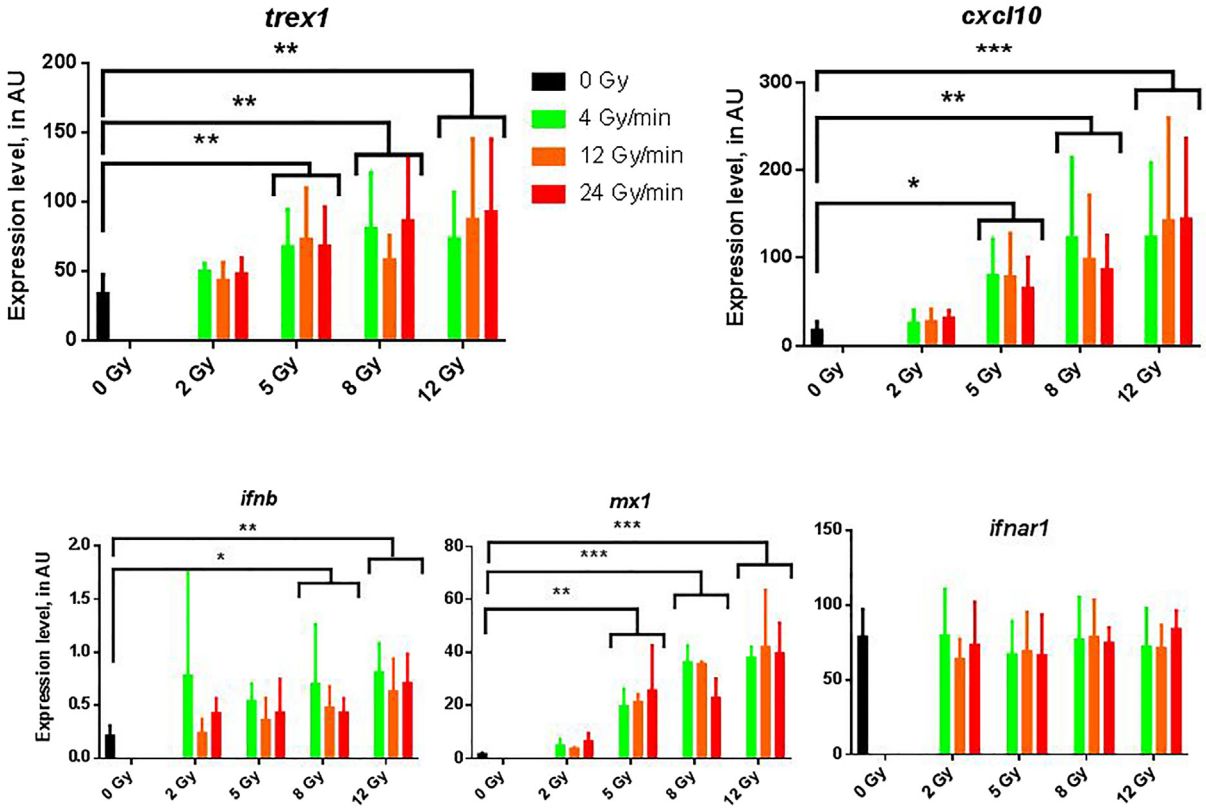

Fig. 2. Representation of the expression of genes involved in the type I interferon pathway after RT *in-vitro* at various doses and dose-rates. Results of RTqPCR experiments for the expression of genes trex1 (antagonist of type I interferon pathway), cxcl10, ifnb, mx1 and ifnar1 (agonists and effectors). Data expressed in arbitrary units (AU), medians with interquartile ranges. N = 6 experiments for each condition. Comparisons performed using a non-parametric Mann-Whitney test. * $p < 0.05$; ** $p < 0.01$; *** $p < 0.001$.

Notably, 48 h after RT, we have not shown any difference according on RT dose-rate in the expression of all genes tested, whereas the expressions of *trex1, cxcl10 and mx1* were significantly increased for doses of RT up to 5 Gy and the expression of *ifnb* for doses up to 8 Gy in both of irradiated groups (HDR and LDR) in comparison with the control group, thus confirming the substantial influence RT has on the induction of type I interferon pathway.

3.1.2. Comparison of RT in FFF high-dose rate and in standard low-dose rate in the induction of immunogenic cell-death events

The Fig. 3 represents the results of HMGB1 quantification in supernatants by ELISA in ratios to un-irradiated/control condition. Although a substantial increase in amount of HMGB1 was showed for doses of RT up to 5 Gy in comparison with a standard dose of 2 Gy (5 Gy: 1.34 [1.08; 2.62]; 2 Gy: 1.07 [0.7;1.2]; p = 0.002), we have not highlighted any difference in HMGB1 secretion by irradiated CT26 cells according to dose-rate condition, HDR or LDR, for each dose delivered.

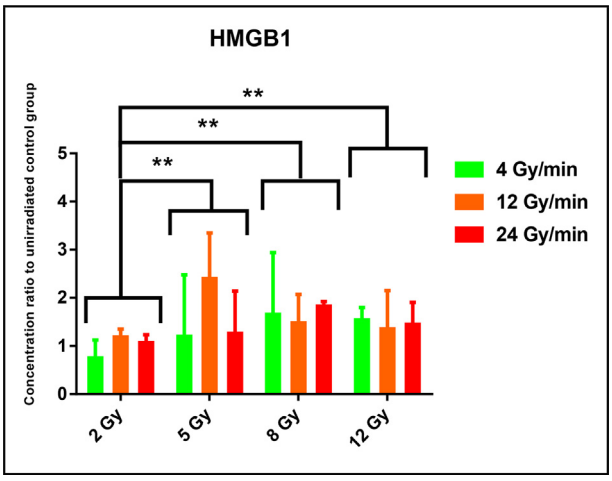

Fig. 3. Secretion of high-mobility group box 1 (HMGB1) protein after RT *in-vitro*, according to the dose delivered and the dose-rate used. HMGB1 concentrations quantified by ELISA test. N = 6 experiments for each condition. Data represented in ratios of HMGB1 concentrations to un-irradiated control group, in medians with interquartile ranges. Comparisons performed using a non-parametric Mann-Whitney statistical test. ** $p < 0.01$.

3.2. In-vivo experiments:

3.2.1. CT26 tumor growth profile in immunocompetent Balb/c mice

We represent in Fig. 4 the tumor growth profile of CT26 tumors. The mean time to reach a tumor volume up to 1500 mm^3 did not appear significantly different between mice receiving 16.5 Gy in HDR or in LDR conditions (HDR: 39.4 days [34.23; 44.57]; LDR: 36 days [28.8; 43.2]; p = 0.39). Moreover, as a confirmation of validity of this experiment, both HDR ($p < 0.001$) and LDR (p = 0.018) groups showed significantly slowed down tumor growth profiles compared to control group (24.86 days [20.01; 29.7]).

3.2.2. Composition of immune cell infiltrates into peritumoral environment after RT in FFF high-dose rate and in standard low-dose rate:

The results of immunomonitoring experiments practiced at J7 after irradiation are detailed in Tables 2 and 3 and represented in Supplementary Fig. 2. No difference was highlighted in ratios of T lymphocytes, CD4+, CD8+, NK, and Treg in total cells between both irradiation conditions. However, such significant differences were

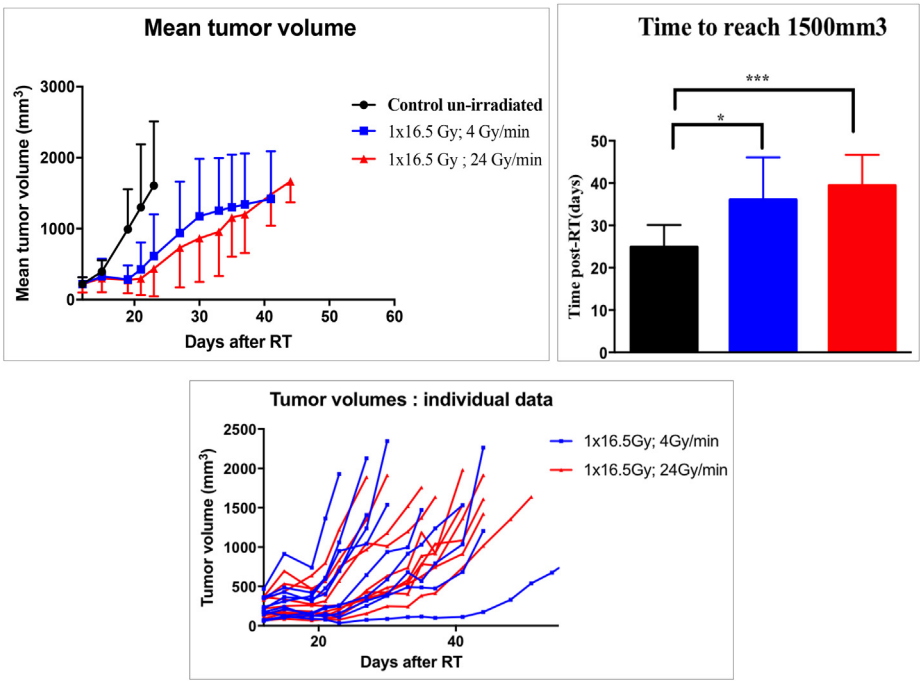

Fig. 4. Tumor-growth profile of CT26 tumors after RT in 24 Gy/min (High-dose rate) versus 4 Gy/min (Standard Low-dose rate). N = 10 mice for each group. Times to reach 1500 mm3 expressed in means with standard deviations. Comparisons performed using a non-parametric Mann-Whitney test. * p < 0.05; *** p < 0.001.

Table 2
Composition of immune microenvironment after RT in high-dose rate using flattening filter-free beams versus standard low-dose rate:

	T lymphocytes	T CD8 + lymphocytes	T CD4 + lymphocytes	NK lymphocytes	Treg lymphocytes
Control	3.26% [2.67; 6.81]	1.35% [1.02; 2.4]	1.37% [1.19; 2.87]	2.34% [2.13; 3.41]	0.38% [0.15; 0.77]
LDR (4 Gy/min)	19.2% [11.16; 26.71]	14.01% [8.85; 21.16]	3.84% [3.29; 4.86]	9.97% [8.93; 12.35]	2.21% [1.18; 2.67]
HDR (24 Gy/min)	17.56% [16.03; 25.33]	14.99% [8.83; 23.24]	3.94% [3.31; 6.48]	8.49% [6.97; 11.27]	1.79% [1.1; 2.11]
HDR VS LDR	p = 0.83	p = 0.84	p = 0.83	p = 0.36	p = 0.4
LDR VS Control	**p = 0.011**	**p = 0.01**	**p = 0.02**	**p = 0.002**	**p = 0.003**
HDR VS Control	**p = 0.006**	**p = 0.01**	**p = 0.011**	**p = 0.03**	**p = 0.03**

Percentages of various cellular types among total cells in CT26 tumor microenvironment, explored by flow cytometry at J7 after a single fraction of 16.5 Gy. All results represented in medians with interquartile range. Data compared using a Mann-Whitney non-parametric test. N = 5 samples for each condition. LDR: standard low-dose rate; HDR: High-dose rate.

Table 3
Prevalence of immune checkpoints within CD8 + T lymphocytes in tumor microenvironment after RT in high-dose rate using flattening filter-free beams versus standard low-dose rate.

	PD1	TIGIT	Tim3	LAG3	PDL1
Control	58.04% [36.23; 61.35]	28.23% [25.54; 39.03]	9.41% [6.65; 10.71]	29.2% [24.75; 49.19]	1.72% [0.99; 5.14]
LDR (4 Gy/min)	85.69% [82.76; 91.41]	50.99% [42.47; 62.27]	22.61% [17.44; 28.31]	41.95% [38.75; 57.6]	47.51% [37.14; 48.43]
HDR (24 Gy/min)	90.08% [75.07; 91.81]	56.59% [44.95; 62.3]	23.68% [20.19; 27.89]	46.52% [36.64; 58.47]	56.09% [29.84; 59.01]
HDR VS LDR	p = 0.72	p = 0.89	p = 0.86	p = 0.89	p = 0.72
LDR VS Control	**p = 0.013**	**p = 0.024**	**p = 0.017**	p = 0.23	**p = 0.013**
HDR VS Control	**p = 0.005**	**p = 0.016**	**p = 0.01**	p = 0.18	**p = 0.005**

Proportion of CD8 + T lymphocytes expressing immune checkpoints within tumor microenvironment of CT26 tumors at J7 post-irradiation. Results for PD1, TIGIT, Tim3 and LAG3 expressed in percentages among T CD8 + lymphocytes. Result for PDL1 expressed in percentage among tumor cells. All results presented in medians with interquartile ranges. Data comparisons done using a Mann-Whitney non-parametric test. N = 5 samples for each condition. LDR: Low-dose rate; HDR: High-dose rate.

observed between both irradiated groups and the control unirradiated condition, thus confirming the ability of RT to increase the part of these cell populations among total cells regardless to the dose-rate used.

3.2.3. Study of transcriptomic profiles based on RNA sequencing analysis

In Fig. 5 we present in an overview heatmap the results of RNA-sequencing performed at J7 post-RT. After comparing LDR and HDR conditions, we did not find any difference in the expression of immune checkpoints PD1, PDL1, TIGIT, Tim3 and PDL2 among total cells in CT26 tumors. As well as for the immunomonitoring experiments, significant differences in the expression of above-mentioned immune-checkpoints were shown between both irradiated conditions (HDR or LDR) and the unirradiated control group.

4. Discussion

This work represents the first study so far examining the potential influence of external beam RT delivered in FFF HDR usable in

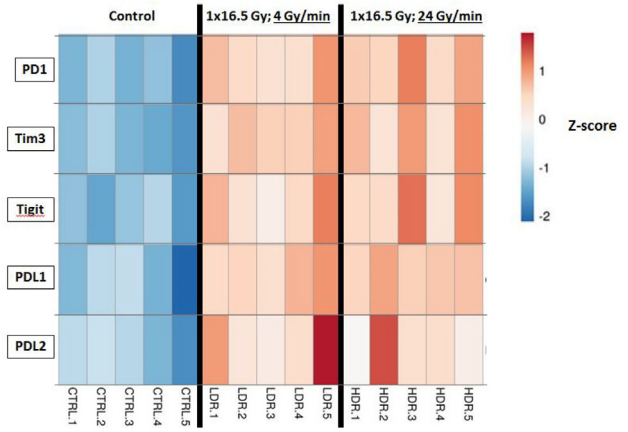

Fig. 5. Expression of immune checkpoints in CT26 tumors after RT *in-vivo* at 24 Gy/min (High-dose rate) versus 4 Gy/min (Standard Low-dose rate). RNA sequencing analysis performed 7 days after RT from tumors RNA. Results presented in Z-scores. CTRL: Control; LDR: Low-dose rate; HDR: High-dose rate.

clinical practice on anti-tumor immunity. Indeed, several experiments done so far were interested in studying FLASH irradiation [27,28], resulting in ultra-high dose rate RT delivery and currently involved only in a beginning clinical practice [29]. On the contrary, FFF beams are already used in patients for the reasons described in the introduction. Thus, in the current context of ever-expanding number of clinical trials involving an association between an immune-checkpoint blockade and an external irradiation, it seemed essential to determine how FFF moderate HDR RT could modify anti-tumor immune response or not, in comparison with RT delivered in standard LDR.

First, concerning the *in-vitro* experiments, we attached importance to studying the type I interferon pathway because of its immunogenic properties that made it a pillar in anti-tumor immune response. We have proved a strict equivalence in the ability of RT to induce this pathway whether it is delivered in LDR or in FFF HDR. By showing an induction of TREX1 exonuclease and IFNB for doses up to 5 Gy, we agreed with the conclusions of Vanpouille-Box et al. [13] who explored it in several models, syngeneic tumors or patient-derived xenografts. However, using RT-qPCR for the analysis of the expression of the ISGs, despite the accuracy of this technique, did not enable us to have an insight about post-translational rearrangements possibly impacting the functionality of subsequent proteins.

Regarding immune cell death, HMGB1 secretion did not differ according to the dose-rate chosen. The increase in HMGB1 secretion for doses up to 5 Gy seems congruent with the work of Chen and al. [30] on pancreatic cancer cells. However, even it is of substantial interest, the secretion of HMGB1 cannot be considered as the only marker of ICD and other criteria such as calreticulin translocation or ATP secretion will have to be the field for further explorations.

Then, about the *in-vivo* experiments, we highlighted the significant part of effector-cell populations such as T CD8 + or NK, the induction after RT of which is already established [31,32]. On the other hand, the improved proportion of immunosuppressive Treg lymphocytes after RT was similar than in relevant published works [14]. Moreover, even if FFF HDR irradiation failed to show a differential induction of widely targeted immune checkpoints PD1, PDL1, Tim3, and TIGIT in comparison with LDR irradiation, those were induced compared to control group, which broadens the concept of RT-inducible checkpoints behind breakthrough clinical trials, published or on-going [33]. Our work represents the first study so far to question the impact of dose-rate on the composition of immune cell infiltrates or on the induction of immune checkpoints within tumor microenvironment.

However, this work is to be continued. Some shortcomings of our methodology lie in the fact that we have experimented with a single tumor model, and that we have not carried out additional work consisting in associating immune checkpoints inhibitors to a radiotherapy delivered in FFF moderate high dose rate in order to highlight a hypothetic difference in tumor growth profile. As it is of evidence that RT alone is insufficient to ensure of the induction of a robust anti-tumor immune response, an on-going study by our research team is of major interest, as it will associate RT with concurrent administration of chemotherapy and immune checkpoint blockades, which represent two additional major contributors to the induction of a strong anti-tumor immune response.

Finally, it is worth notable that we did not include ultra-high dose rate (also called FLASH-RT) into these experiments, thus focusing our attention on FFF high-dose rate which is, on the contrary of FLASH-RT, already involved in stereotactic body radiotherapy for many patients treated in various locations. Some studies evaluating the impact of FLASH-RT on anti-tumor immune response are expected, as this technique of ultra-high dose rate represents a promising issue in a foreseeable future.

5. Conclusion

In this original work, we did not highlight a significant difference in relevant fields of anti-tumor immune response between RT delivered in conventional dose-rate and in FFF high-dose rate. Subject to reproducibility of these results in other syngeneic models, this should make numerous research protocols associating immune checkpoint blockades with external RT fit with using moderate HDR RT using FFF beams, thus contributing to their utilization in routine [34].

Overall, considering these experiments in a single tumor model, and all the existing literature reporting an absence of additional toxicity caused by FFF HDR, this technique seems at least not deleterious for the induction of major pathways involved in the anti-tumor immune response, and therefore can be implemented into clinical daily practice, however with caution.

This work nevertheless needs to be improved with the exploration of some other aspects of immune cell death process (calreticulin), and with the use of immune checkpoints blockades in *in-vivo* experiments with the goal of exploring a potential benefic association with FFF moderate high-dose RT. These complementary works will be the field for future publications.

Declaration of Competing Interest

The authors declare that they have no known competing financial interests or personal relationships that could have appeared to influence the work reported in this paper.

Acknowledgments

We thank the ARC Cancer Foundation and the “Conseil Régional Bourgogne Franche-Comte” for the confidence they have shown in us by granting us funding for this research, and the Georges-François Leclerc Cancer Centre for its support. The dosimetry and splinting device development work was funded by the IMODI Consortium.

Appendix A. Supplementary data

Supplementary data to this article can be found online at https://doi.org/10.1016/j.ctro.2020.07.004.

References

[1] Tsang MWK. Stereotactic body radiotherapy: current strategies and future development. J Thorac Dis 2016;8(S6):S517–27. https://doi.org/10.21037/jtd.2016.03.14.

[2] Petrelli F, Comito T, Ghidini A, Torri V, Scorsetti M, Barni S. Stereotactic body radiation therapy for locally advanced pancreatic cancer: a systematic review and pooled analysis of 19 trials. Int J Radiation Oncol Biol Phys 2017;97(2):313–22. https://doi.org/10.1016/j.ijrobp.2016.10.030.

[3] Tree AC, Khoo VS, Eeles RA, et al. Stereotactic body radiotherapy for oligometastases. Lancet Oncol 2013;14(1):e28–37. https://doi.org/10.1016/S1470-2045(12)70510-7.

[4] Rosenblatt E. Planning national radiotherapy services. Front Oncol 2014;4. https://doi.org/10.3389/fonc.2014.00315.

[5] Dahele M, Slotman B, Verbakel W. Stereotactic body radiotherapy for spine and bony pelvis using flattening filter free volumetric modulated arc therapy, 6D cone-beam CT and simple positioning techniques: Treatment time and patient stability. Acta Oncol 2016;55(6):795–8. https://doi.org/10.3109/0284186X.2015.1119885.

[6] Kragl G, Wetterstedt S, Knäusl B, et al. Dosimetric characteristics of 6 and 10MV unflattened photon beams. Radiotherapy Oncol 2009;93(1):141–6. https://doi.org/10.1016/j.radonc.2009.06.008.

[7] Gasic D, Ohlhues L, Brodin NP, et al. A treatment planning and delivery comparison of volumetric modulated arc therapy with or without flattening filter for gliomas, brain metastases, prostate, head/neck and early stage lung cancer. Acta Oncol 2014;53(8):1005–11. https://doi.org/10.3109/0284186X.2014.925578.

[8] Spiotto M, Fu Y-X, Weichselbaum RR. The intersection of radiotherapy and immunotherapy: Mechanisms and clinical implications. Sci Immunol 2016;1(3). https://doi.org/10.1126/sciimmunol.aag1266. eaag1266-eaag1266.

[9] Golden EB, Apetoh L. Radiotherapy and immunogenic cell death. Seminars Radiation Oncol 2015;25(1):11–7. https://doi.org/10.1016/j.semradonc.2014.07.005.

[10] Burnette BC, Liang H, Lee Y, et al. The efficacy of radiotherapy relies upon induction of type I interferon-dependent innate and adaptive immunity. Cancer Res 2011;71(7):2488–96. https://doi.org/10.1158/0008-5472.CAN-10-2820.

[11] Lim JYH, Gerber SA, Murphy SP, Lord EM. Type I interferons induced by radiation therapy mediate recruitment and effector function of CD8+ T cells. Cancer Immunol Immunother 2014;63(3):259–71. https://doi.org/10.1007/s00262-013-1506-7.

[12] Sistigu A, Yamazaki T, Vacchelli E, et al. Cancer cell–autonomous contribution of type I interferon signaling to the efficacy of chemotherapy. Nat Med 2014;20(11):1301–9. https://doi.org/10.1038/nm.3708.

[13] Vanpouille-Box C, Alard A, Aryankalayil MJ, et al. DNA exonuclease Trex1 regulates radiotherapy-induced tumour immunogenicity. Nat Commun 2017;8:15618. https://doi.org/10.1038/ncomms15618.

[14] Muroyama Y, Nirschl TR, Kochel CM, et al. Stereotactic radiotherapy increases functionally suppressive regulatory T cells in the tumor microenvironment. Cancer Immunol Res 2017;5(11):992–1004. https://doi.org/10.1158/2326-6066.CIR-17-0040.

[15] Vatner RE, Formenti SC. Myeloid-derived cells in tumors: effects of radiation. Seminars Radiation Oncol 2015;25(1):18–27. https://doi.org/10.1016/j.semradonc.2014.07.008.

[16] Grapin M, Richard C, Limagne E, et al. Optimized fractionated radiotherapy with anti-PD-L1 and anti-TIGIT: a promising new combination. J Immunotherapy Cancer 2019;7(1):160. https://doi.org/10.1186/s40425-019-0634-9.

[17] Sørensen BS, Vestergaard A, Overgaard J, Præstegaard LH. Dependence of cell survival on instantaneous dose rate of a linear accelerator. Radiother Oncol 2011;101(1):223–5. https://doi.org/10.1016/j.radonc.2011.06.018.

[18] King RB, Hyland WB, Cole AJ, et al. Anin vitrostudy of the radiobiological effects of flattening filter free radiotherapy treatments. Phys Med Biol 2013;58(5):N83–94. https://doi.org/10.1088/0031-9155/58/5/N83.

[19] Cerviño LI, Soultan D, Advani SJ, et al. An *in vitro* study for the dosimetric and radiobiological validation of respiratory gating in conventional and hypofractionated radiotherapy of the lung: effect of dose, dose rate, and breathing pattern. Phys Med Biol 2019;64(13):. https://doi.org/10.1088/1361-6560/ab2940135009.

[20] Lasio G, Guerrero M, Goetz W, Lima F, Baulch JE. Effect of varying dose-per-pulse and average dose rate in X-ray beam irradiation on cultured cell survival. Radiat Environ Biophys 2014;53(4):671–6. https://doi.org/10.1007/s00411-014-0565-2.

[21] Sarojini S, Pecora A, Milinovikj N, et al. A combination of high dose rate (10X FFF/2400 MU/min/10 MV X-rays) and total low dose (0.5 Gy) induces a higher rate of apoptosis in melanoma cells in vitro and superior preservation of normal melanocytes. Melanoma Res 2015;25(5):376–89. https://doi.org/10.1097/CMR.0000000000000174.

[22] Dang TM, Peters MJ, Hickey B, Semciw A. Efficacy of flattening-filter-free beam in stereotactic body radiation therapy planning and treatment: a systematic review with meta-analysis. J Med Imaging Radiation Oncol 2017;61(3):379–87. https://doi.org/10.1111/1754-9485.12583.

[23] Végran F, Berger H, Boidot R, et al. The transcription factor IRF1 dictates the IL-21-dependent anticancer functions of TH9 cells. Nat Immunol 2014;15(8):758–66. https://doi.org/10.1038/ni.2925.

[24] Bugaut H, Bruchard M, Berger H, et al. Bleomycin exerts ambivalent antitumor immune effect by triggering both immunogenic cell death and proliferation of regulatory T cells. Glod JW, ed.. PLoS ONE 2013;8(6). https://doi.org/10.1371/journal.pone.0065181. e65181.

[25] Wolf M, Lossdörfer S, Römer P, et al. Short-term heat pre-treatment modulates the release of HMGB1 and pro-inflammatory cytokines in hPDL cells following mechanical loading and affects monocyte behavior. Clin Oral Invest 2016;20(5):923–31. https://doi.org/10.1007/s00784-015-1580-7.

[26] Subramanian A, Tamayo P, Mootha VK, et al. Gene set enrichment analysis: a knowledge-based approach for interpreting genome-wide expression profiles. Proc Natl Acad Sci 2005;102(43):15545–50. https://doi.org/10.1073/pnas.0506580102.

[27] Favaudon V, Caplier L, Monceau V, et al. Ultrahigh dose-rate FLASH irradiation increases the differential response between normal and tumor tissue in mice. Sci Transl Med 2014;6(245). https://doi.org/10.1126/scitranslmed.3008973. 245ra93-245ra93.

[28] Vozenin M-C, Fornel PD, Petersson K, et al. The advantage of FLASH radiotherapy confirmed in mini-pig and cat-cancer patients. Clin Cancer Res 2019;25(1):35–42. https://doi.org/10.1158/1078-0432.CCR-17-3375.

[29] Bourhis J, Sozzi WJ, Jorge PG, et al. Treatment of a first patient with FLASH-radiotherapy. Radiother Oncol 2019;139:18–22. https://doi.org/10.1016/j.radonc.2019.06.019.

[30] Chen X, Zhang L, Jiang Y, et al. Radiotherapy-induced cell death activates paracrine HMGB1-TLR2 signaling and accelerates pancreatic carcinoma metastasis. J Exp Clin Cancer Res 2018;37(1):77. https://doi.org/10.1186/s13046-018-0726-2.

[31] Matsumura S, Wang B, Kawashima N, et al. Radiation-induced CXCL16 release by breast cancer cells attracts effector T cells. J Immunol 2008;181(5):3099–107. https://doi.org/10.4049/jimmunol.181.5.3099.

[32] Eckert F, Schilbach K, Klumpp L, et al. Potential role of CXCR4 targeting in the context of radiotherapy and immunotherapy of cancer. Front Immunol 2018;9:3018. https://doi.org/10.3389/fimmu.2018.03018.

[33] Antonia SJ, Villegas A, Daniel D, et al. Durvalumab after chemoradiotherapy in stage III non–small-cell lung cancer. N Engl J Med 2017. https://doi.org/10.1056/NEJMoa1709937.

[34] Galon J, Bruni D. Approaches to treat immune hot, altered and cold tumours with combination immunotherapies. Nat Rev Drug Discov 2019;18(3):197–218. https://doi.org/10.1038/s41573-018-0007-y.